AAS 14-052

ADAPTIVE AUGMENTING CONTROL FLIGHT CHARACTERIZATION EXPERIMENT ON AN F/A-18

Tannen S. VanZwieten[*], Eric T. Gilligan[†], John H. Wall[‡], Jeb S. Orr[§], Christopher J. Miller[¶] and Curtis E. Hanson[‖]

The NASA Marshall Space Flight Center (MSFC) Flight Mechanics and Analysis Division developed an Adaptive Augmenting Control (AAC) algorithm for launch vehicles that improves robustness and performance by adapting an otherwise well-tuned classical control algorithm to unexpected environments or variations in vehicle dynamics. This AAC algorithm is currently part of the baseline design for the SLS Flight Control System (FCS), but prior to this series of research flights it was the only component of the autopilot design that had not been flight tested. The Space Launch System (SLS) flight software prototype, including the adaptive component, was recently tested on a piloted aircraft at Dryden Flight Research Center (DFRC) which has the capability to achieve a high level of dynamic similarity to a launch vehicle. Scenarios for the flight test campaign were designed specifically to evaluate the AAC algorithm to ensure that it is able to achieve the expected performance improvements with no adverse impacts in nominal or near-nominal scenarios. Having completed the recent series of flight characterization experiments on DFRC's F/A-18, the AAC algorithm's capability, robustness, and reproducibility, have been successfully demonstrated. Thus, the entire SLS control architecture has been successfully flight tested in a relevant environment. This has increased NASA's confidence that the autopilot design is ready to fly on the SLS Block I vehicle and will exceed the performance of previous architectures.

1 INTRODUCTION

In-house development of an AAC algorithm for launch vehicles as an addition to the classical control architecture began at NASA MSFC during the Constellation Program. Development of the adaptive algorithm was accelerated during the current SLS Program where the NASA community has continued to develop confidence in the algorithm through extensive internal and external reviews, stability analysis, flight software implementation and testing, time and frequency-domain analysis of failure scenarios, and Monte Carlo analysis. Maturation of the algorithm coupled with the demonstration of tangible, repeatable benefits led to it being baselined as part of the autopilot design and flight software build prior to the SLS Preliminary Design Review in 2013.

[*] SLS Flight Controls Lead, Control Systems Design & Analysis Branch, NASA MSFC, Huntsville, AL, 35812
[†] Aerospace Engineer, Control Systems Design & Analysis Branch, NASA MSFC, Huntsville, AL, 35812
[‡] SLS Flight Controls Deputy Lead, Guidance, Navigation, & Control Group; Dynamic Concepts, Inc. (Jacobs ESSSA Group), Huntsville, AL, 35806
[§] Senior Member of the Technical Staff, Dynamics & Control; The Charles Stark Draper Laboratory, Inc. (Jacobs ESSSA Group), Huntsville, Alabama, 35806
[¶] FAST Chief Engineer, Flight Controls & Dynamics Branch, NASA DFRC, Edwards, CA, 93523
[‖] Aerospace Engineer, Flight Controls & Dynamics Branch, NASA DFRC, Edwards, CA, 93523

The SLS family of vehicles (see Figure 1) will deliver more payload to orbit and produce more thrust than any other vehicle, past or present, opening the way to new frontiers of space exploration. Like all large launch vehicles SLS must balance the competing needs of maximizing performance while maintaining robustness. With its high thrust, large size and multiple elements, SLS exhibits a highly flexible structure with non-planar bending characteristics. Control commands must be allocated to each of its six engines which are actuated along pitch and yaw axes by thrust vector control systems with limited bandwidth. Each of its six engines are actuated along two axes by thrust vector control systems, leading to a control allocation and bandwidth management challenge. The massive propellant tanks have lightly damped lateral sloshing modes and the uncertain payload envelope comes with its own set of parasitic dynamics. The SLS trajectories are highly optimized to squeeze every bit of performance out of the rocket, which further challenges the flight control design and leaves very little margin to share across all of the disciplines and subsystems.

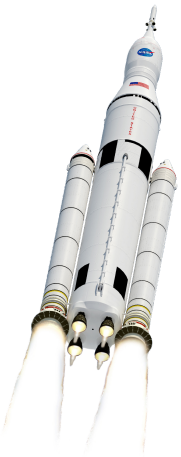

Figure 1. SLS Block I Vehicle

Figure 2. F/A-18 FAST

In the current fast-paced, low cost development environment there is not only a need for creativity and innovation from a design perspective, but a need for new technologies to be coupled with inexpensive, quick turn-around testing options. Testing the SLS FCS on a small-scale launch vehicle or a sounding rocket would require the SLS software to be tailored to the existing vehicle specifications, including a re-optimization of the control parameters to provide the experimental platform with adequate closed-loop attitude tracking. Additionally, these platforms lack key features of the SLS dynamics, such as low-frequency bending modes, that are needed to thoroughly evaluate the adaptive law. Implementation on a piloted aircraft quickly became an attractive alternative since DFRC had developed an F/A-18 Full-Scale Advanced Systems Testbed (FAST), shown in Figure 2, capable of matching the dynamics of a reference model and accommodating a variety of control experiments. Furthermore, this platform allowed for substiantially longer flight times, multiple experimental setups, and more data collection. Thus, the tests were conducted using the actual SLS flight software prototype under SLS-based scenarios, which thought it was flying SLS. Within a year of the concept study, a series of flight experiments were completed in November and December of 2013 on an F/A-18, Tail Number (TN) 853. This was part of the process to verify and validate the Space Launch System (SLS) baseline control design with emphasis on fully exercising the AAC component, the only component of the control system which had not been previously flight tested.

This paper is organized as follows. Section 2 provides a brief overview of the SLS Adaptive

Augmenting Control system with emphasis on its design philosophy and key characteristics. Section 3 then follows with a description of the motivation for the SLS Program to complete specific research flight objectives. The experimental setup is described in Section 4, including features of the F/A-18 research aircraft that makes it an ideal platform for this experiment in Section 4.1. It also includes a description of how the trajectory was defined (Section 4.2) and method that was used for achieving attitude matching between the aircraft and SLS (Section 4.3), including the injection of high-frequency content to impose unstable launch vehicle parasitic dynamics on the rigid body. Modifications to the SLS flight software prototype for implementation as part of the flight experiment are described in Section 4.4. Finally, a description of the flights and the test cases which were completed along with sample results are provided in Section 5 before making some concluding remarks.

2 OVERVIEW OF THE SLS ADAPTIVE AUGMENTING CONTROL ALGORITHM

The AAC scheme was designed to improve launch vehicles robustness and performance by adapting an otherwise well-tuned classical control algorithm to unexpected environments or variations in vehicle dynamics. The original motivation for considering the development and inclusion of an advanced control approach specifically for human-rated launch vehicles did not result from a failure of the traditional fixed gain control design, since GN&C issues are rarely the cause for launch vehicle failures.[1] In fact, in the absence of vehicle or environmental uncertainty, a fixed-gain controller could be optimized prior to flight such that there would be no motivation for adaptation. However, a review of historical launch vehicle data from 1990 to 2002 revealed that 41% of failures in other subsystems might have been mitigated by advanced GN&C technologies.[1] Control approaches that use real-time adaptation thrive when there are environmental or vehicle model uncertainties, including in-flight anomalies and failure scenarios. Additional factors that are particularly relevant for human-rated systems include code complexity, predictability of the response, and ability to reconcile the stability analysis in the context of classical gain and phase margin. In other words, a "black box" approach with numerous adaptive gains, complex nonlinearities, and no way of estimating classical stability margins would naturally be difficult to justify from a risk perspective, even if its performance exceeded that of the existing architecture.

The philosophy which drove the formulation of the AAC algorithm, its initial testing during Constellation,[2] and its refinement as part of the baseline autopilot design for NASA's Space Launch System (SLS)[3,4] was first and foremost to maintain nominal system performance and be compatible to some extent with classical stability criteria. Thus, an adaptive system was developed with a predictable response that augments the existing control architecture and protects the nominal control gains. Secondly, the philosophy was to provide additional robustness using a simple architecture that could recover from poor performance and prevent or delay loss of vehicle (LOV). To effectively accomplish this, typical model reference adaptive control logic was used within the adaptive update law to increase the control gain when excessive tracking error indicates that performance is low. An additional term was included which decreases the adaptive gain when excessive frequency content is observed in the control command as a result of launch vehicle parasitic dynamics (flexibility, fuel slosh, and actuators). The gain decrease element is a departure from traditional adaptive control approaches, which typically improve performance by increasing the magnitude of the adaptive gain in response to tracking error.

The resulting AAC algorithm is a forward loop gain multiplicative adaptive algorithm that modifies the total attitude control system gain in response to sensed model errors or undesirable parasitic

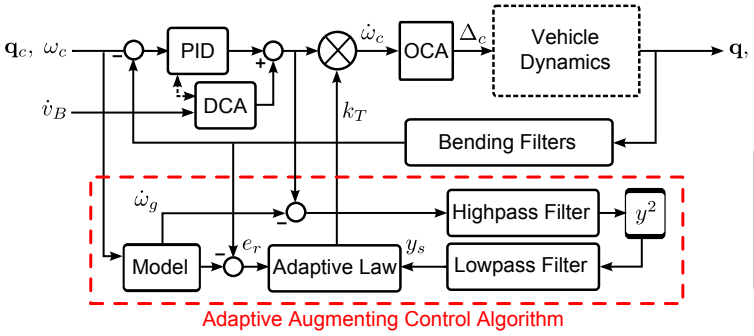

Figure 3. Block Diagram of the SLS FCS with AAC

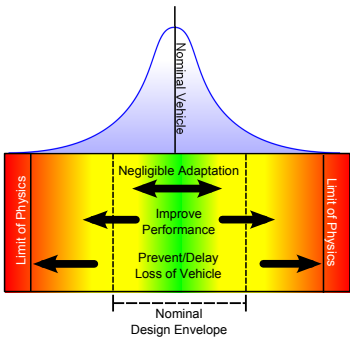

Figure 4. AAC Design Philosophy

mode resonances (see Figure 3). It improves or decreases performance by balancing attitude tracking with the mitigation of undesirable frequency content in the control path. In the case of the latter, this is often due to unmodeled or mismodeled parasitic dynamics that would otherwise result in a closed-loop instability or a potentially destructive limit cycle. In this case the adaptive controller responds to the frequency content in the control signal by decreasing the total loop gain to reduce the interaction between these dynamics and the controller. The AAC algorithm is computationally simple and has stability properties that are reconcilable in the context of classical frequency-domain criteria (i.e., gain and phase margin). The algorithm assumes that the fixed-gain attitude control design is well-tuned for a nominal vehicle and trajectory which means that adaptation should only be needed outside of the nominal design envelope, as depicted in Figure 4. Therefore, by design the adaptive gain multiplie are attracted to unity (no impact to the fixed-gain response) and adaptation only occurs on an as-needed basis. Furthermore, the adaptation is attracted to the nominal design and adapts only on an as-needed basis. Its characteristics in simulation reflect the algorithm's three summary-level objectives:

1. "Do no harm;" return to baseline control design when not needed.
2. Increase performance; respond to error in ability of vehicle to track commands.
3. Regain stability; respond to undesirable control-structure interaction or other parasitic dynamics.

3 MOTIVATION FOR FLIGHT TESTING THE ADAPTIVE AUGMENTING CONTROLLER

This MSFC algorithm reached a high maturity level as part of the SLS autopilot design through simulation-based development and internal and external analytical review. However, leading into the SLS Program Preliminary Design Review, AAC remained the only component of the SLS autopilot design that had not yet been flight tested. Completion of the testing described in this paper means that every algorithm in the SLS control design architecture has been successfully demonstrated in flight at least once as shown in Figure 5.

3.1 Objectives of the Research Flights

The DFRC F/A-18 FAST was used as a platform for conducting a flight characterization experiment intended to validate that the algorithm achieves the purposes for which it was designed.

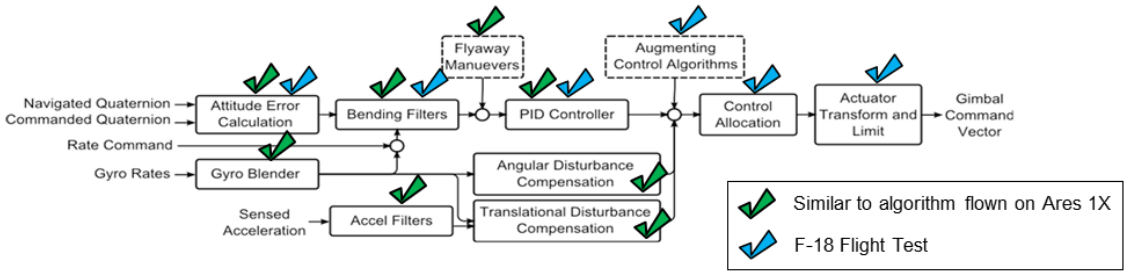

Figure 5. Flight Testing of the SLS Autopilot Flight Software Prototype

Additionally, in consideration of the current SLS requirement to incorporate manual steering capability it is desirable to understand the interaction between a pilot and the AAC. Thus, the primary objectives of the research flights are summarized as follows:

1. Demonstrate closed-loop tracking with negligible adaptation in an environment that is commensurate with the nominal controller design envelope.
2. Demonstrate improved performance in an environment where the nominal controller performance is less than desired.
3. Demonstrate the ability to recover from unstable, mis-modeled parasitic dynamics to a bounded non-destructive limit cycle.
4. Explore interactions between manual steering and the AAC.

The approach for achieving these objectives was to develop multiple SLS scenarios which consider physically realizable normal and failure conditions that map into Objectives 1-3. An additional test case was developed to demonstrate Objective 3 by staging control-structure interaction with the physical resonance of the F/A-18 airframe itself. In order to achieve Objective 4, a subset of these scenarios were repeated with the pilot providing attitude tracking.

Additional design considerations to enhance the value of the results were to maximize dynamic similarity between the aircraft and SLS pitch attitude error dynamics, incorporate as much of the SLS FCS as possible to capture its interactions with AAC, and force the AAC to respond to injected parasitic dynamics outside of the aircraft's software package when possible. The experiment development process was also structured to allow the SLS controls engineers to gain valuable insight toward the software integration and flight certification of the full-scale algorithm. In addition to validating the AAC in conjunction with the fixed-gain portion of the FCS, the process of developing test cases in a MSFC simulation environment, testing each of them in the DFRC F/A-18 hardware-in-the-loop simulation, and then capturing flight test results allowed for verification that the flight software performed as expected.

4 EXPERIMENT SETUP

Combining the high value of testing AAC in a relevant environment with the need for an affordable testing option led to the unconventional approach of conducting flight tests on a research aircraft. Controls experiments have been supported previously on Dryden's F/A-18, but this is the

first time the aircraft was considered for testing an algorithm specifically designed and tuned for launch vehicles. To aid the reader in understanding the relevance of the test results, this section provides an overview of the aircraft platform and key features of the implementation for the launch vehicle flight experiment. The following sections do not capture every detail of the implementation, but rather are intended to illustrate at a basic level the relevant aspects of the test platform and implementation for the launch vehicle experiment.

4.1 Applicability of the F/A-18 as a SLS Flight Test Platform

This flight characterization experiment was performed on the F/A-18 (TN 853) FAST platform.[5] This aircraft is maintained by the NASA Dryden Flight Research Center and was developed specifically to accommodate a variety of full-authority controls experiments. Aided by the presence of a qualified research pilot, the F/A-18 TN 853 has an experimental envelope called the Class B envelope (Figure 6) that ensures safe recovery from unusual attitudes and configurations. The favorable recoverability characteristics of the aircraft while inside the Class B envelope allowed DFRC engineers to pre-clear the aircraft for full-authority experimental control while inside the prescribed altitude and Mach constraints. The aircraft itself features production and research sensor inputs, pilot experiment engage/disengage capability, real-time configuration of multiple experiments on a single flight, as well as failure detection with automatic reversion to fail-safe mode. As with the traditional FCS, the experimental controller inside the Class B envelope is able to control ten aerodynamic effectors and two throttles. The aircraft capability was further enhanced through the development and implementation of a nonlinear dynamic inversion controller,[6,7] allowing it to effectively match the attitude dynamics of any system exhibiting a slower response, including SLS.

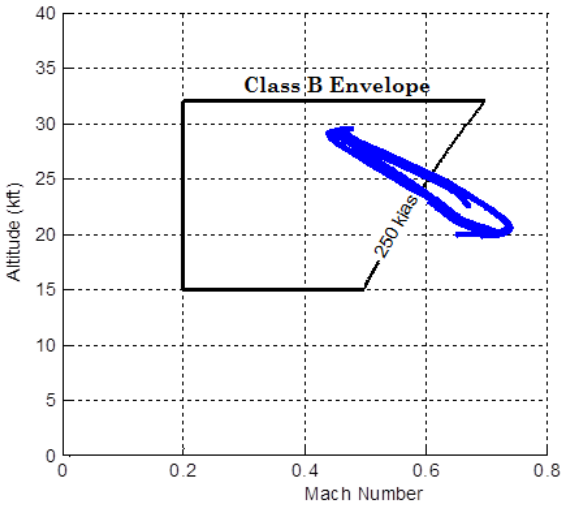

Figure 6. Class B Envelope & Sample Trajectory

The F/A-18 aircraft has relatively high mass and inertia and a large thrust-to-weight ratio, owing to its military heritage. Its high performance provides it with the capability of flying a variety of aggressive trajectories and closely tracking attitude rates commensurate with what will be exhibited by SLS during ascent. Atmospheric disturbances, model uncertainties, and parasitic dynamics may be reproduced by the airframe via the use of primary and secondary control surfaces, including leading and trailing edge flaps, symmetric ailerons, and symmetric rudders. This platform also offers more test maneuvers and longer maneuver times than a single rocket or missile test, which provides ample opportunity to fully and repeatedly exercise all aspects of the SLS AAC algorithm.

4.2 Experiment Trajectory

The aircraft's trajectory was designed to track a pitch rate of approximately 0.75 deg/sec, which is near the average pitch rate of the SLS during its pitch-over maneuver that occurs prior to separation

of the vehicle's Solid Rocket Boosters (SRBs). The experiment was not designed to match the aircraft's pitch attitude to that of SLS, since this would require a near-vertical flight path which is not achievable with an aircraft thrust-to-weight ratio of less than unity. The need to perform the experiment inside the Class B envelope further constrained the aircraft trajectory design since initiating the trajectory at a high pitch attitude would result in the aircraft rapidly losing speed and flying out the left end of the envelope, thereby reducing the time available on each trajectory to perform the controls experiment. Thus, the trajectory was designed to provide pitch rates that closely approximate those of SLS and maximize the experiment time, given the constraints imposed by the Class B envelope. Figure 6 shows a sample trajectory (blue line) that achieves the desired performance within the Class B experimental envelope (black lines) during a simulated flight.

The resulting trajectory design is shown shown in Figure 7. Prior to initiating each test scenario, the pilot accelerates the aircraft to approximately 330 knots (approximately Mach 0.5) and 19,000 ft, then rotates to 35 degree pitch attitude so that the envelope is entered near the bottom right side. Once at the desired altitude, Mach, and pitch attitude the pilot arms and engages the desired SLS experiment. The entrance criteria is not exact and has some impact on the control surface effectiveness and available trajectory time. After the experiment is engaged, the autopilot tracks the desired pitch rate (unless manual steering is engaged). The pilot monitors the experiment and manages aircraft throttle near peak altitude so that it will be slower to accelerate towards the high end of the velocity envelope as it begins its pitch downward. Engine gyroscopic coupling does result in a transient due to the pitch de-throttle, but the pilots were able to ensure a smooth, gradual throttle transition in order to minimize undesirable pitch transients and their subsequent effect on the test results.

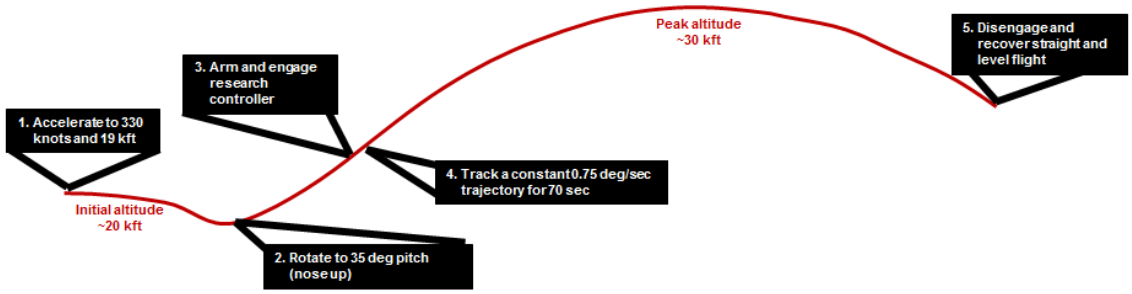

Figure 7. Prescribed Trajectory for the Flight Experiment

Figure 8. Photographs Depicting the Trajectory Flown Repeatedly by the F/A-18

During a typical sortie, trajectories approximately matching the one described in Figure 7 were repeated within the available airspace until fuel constraints required the aircraft to land. Each time the trajectory was repeated during flight, the aircraft was configured with a different SLS test scenario. Photographs taken of FAST performing this trajectory as part of the SLS experiment are shown in Figure 8. Exceptions to the aforementioned trajectory implementation are for (1) manual steering, where the pilot seeks to track the desired attitude rate while performing the experiment, and (2) experiments to detect, excite, and mitigate an airframe structural mode for which the pilot maintained straight-and-level flight, as described in the latter part of Section 5.4.

4.3 Pitch Attitude Matching

The aircraft trajectory described in Figure 7 enables the F/A-18 in conjunction with the FAST Nonlinear Dynamic Inversion (NDI) controller to closely match SLS attitude dynamics and simulate up to a 70 sec window of the SLS trajectory before the aircraft exits the flight envelope, automatically disengaging the experiment. The most challenging SLS dynamics occur between liftoff and separation of the SRBs, where the high dynamic pressure during this endoatmospheric phase requires tight attitude tracking (high controller gain) to retain stability. This must be achieved without exciting parasitic dynamics, which is more challenging when the controller gains are high.

SLS scenarios to be flown on the aircraft were designed using a linear, planar, high-fidelity SLS simulation[8] that used model parameters that were consistent with the program's most recent design analysis cycle (DAC-2) combined with a second-order, time-varying aircraft model with delays that was provided by DFRC. These scenarios and the SLS model were supplied to DFRC, where the model was used to provide an SLS attitude and rate errors as a reference and the existing NDI[6, 7] was modified to better achieve the pitch error dynamics prescribed by the SLS models. Each scenario was verified in the DFRC hardware-in-the-loop simulation (HILS) to adequately match the SLS simulated results as part of a formal Verification and Validation process. In spite of the particularly challenging large magnitude, high frequency content SLS attitude dynamics, the DFRC HILS results matched remarkably well.

Since one of the AAC and corresponding research flight objectives was to detect and mitigate unstable parasitic dynamics if they were to come about unexpectedly during a flight, this presented an additional challenge in regard to attitude matching over what was needed for nominal and low-performance test cases which, in the case of an in-flight anomaly, would exhibit an instability at a much lower frequency. The existing FAST NDI used a combination of primary and secondary control surfaces to track the reference model (in this case, the SLS model), but was redesigned to be able to effect high-frequency attitude dynamics in flight to simulate launch vehicle parasitic dynamics such as sloshing fuel and structural mode resonances. This still resulted in the SLS simulated instability being excited by the same effectors that were used to cancel it. It was more desirable to provide physical separation in the case of simulated flexible body instabilities by implementing the SLS model and control action through the use of different actuators. To this end, the NDI control commands used to re-produce frequency content to match SLS flexible body motion was mapped to the ailerons while the other effectors were used to implement the SLS FCS commands and track the gross aircraft motion.

4.4 SLS Flight Software Prototype Implementation

The FCS design, including parameter gains optimized for SLS, matches those used for DAC-2 (the most recently completed cycle at the onset of this effort) although the AAC component was

updated from the DAC-2 to the DAC-3 implementation as described by Wall et al.[3] There were, however, several changes made to the flight software prototype to facilitate implementation of the flight experiment. Since the FCS has the same form across all axes, the controls experiment was implemented on the pitch-axis only for simplicity. In the operational SLS vehicle, the control allocation framework accounts for the booster thrust vector control system being rotated 45 degrees with respect to the pitch axis. Since this is a pitch-only experiment, the control allocator within the FCS as well as the SLS reference model assumed the TVC system to be in-plane with the pitch axis. The controller was also modified to schedule all gains and parameters with respect to maneuver time rather than other navigated independent variables used in the production system. The SLS FCS includes sensor blending, but this was implemented as part of the plant model instead of the controller since the aircraft uses a single sensor for attitude and rate as opposed to the SLS which requires a blend of multiple sensor measurements to achieve ample attenuation of structural modes. The autopilot's discrete filters were re-discretized from 50 Hz to 80 Hz to accommodate the update rate of the sensors during the experiment. The only part of the SLS autopilot architecture that was disabled was the disturbance compensation algorithm, since its inclusion would unnecessarily complicate the results by responding to the aircraft's translational dynamics that are not controlled by the NDI and therefore not reflective of SLS.

5 SUMMARY OF RESEARCH FLIGHTS AND RESULTS

Two series of flights have been conducted using the SLS autopilot prototype software on the FAST platform. The first series consisted of three flights completed on 14-15 November 2013. During these three flights an F/A-18 structural mode identification test (described in 5.4) was completed while in level flight, along with conducting 45 SLS-like trajectories in autopilot mode which were designed to match pre-defined SLS scenarios. With the high number of trajectories that were completed, AAC design objectives 1-3 had been successfully demonstrated multiple times at the conclusion of the first series of research flights.

During the second flight campaign completed on 11-12 December 2013, the emphasis shifted to mitigating the previously-identified airframe structural dynamics, exploring interactions between manual steering and AAC, and repeating SLS scenarios that had exhibited in-flight variability. Approximately 13 straight-and-level tests were completed to detect and use AAC to mitigate the airframe's structural mode and 40 SLS-like trajectories were flown across two sorties.

A brief description of the SLS scenarios that were flown are provided in Tables 1, 2 and 3 along with which flight test ("FT") they were executed and whether the tests were completed in autopilot mode (denoted "A") or manual steering mode (denoted "M"). Repeats are captured with multiple "A" or "M" designations. F/A-18 airframe system identification tests are marked ("ID") and the subsequent SLS FCS tests with AAC on/off were marked S/L to indicate that they were completed on a straight-and-level flight path. Test cases completed in order to explore interactions between manual steering and the AAC are indicated in the aforementioned tables. Analysis of the results with manual steering are forthcoming and as such are not included in this paper.

5.1 Flight Test Results for Near-Nominal SLS Scenarios (Objective 1)

The first flight objective seeks to show negligible adaptation in an environment that is commensurate with the nominal controller design envelope. Three test cases were flown that map into this objective, as shown in Table 1. Each of the test cases were flown with both AAC on and AAC off for comparison.

Table 1. Flight Tested Objective 1 Scenarios / Test Cases

TC	Description of SLS Scenario	FT1	FT2	FT3	FT4	FT5
0	Nominal Plant, environment & controller	A	A		MM	MM
1	Heavy/slow vehicle			A		
2	Light/fast vehicle			A		

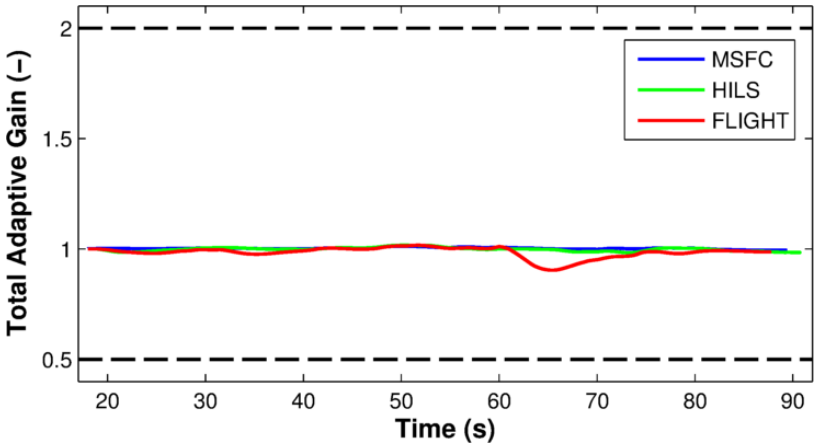

Figure 9. Adaptation of the Total Loop Gain (Nominal SLS Scenario)

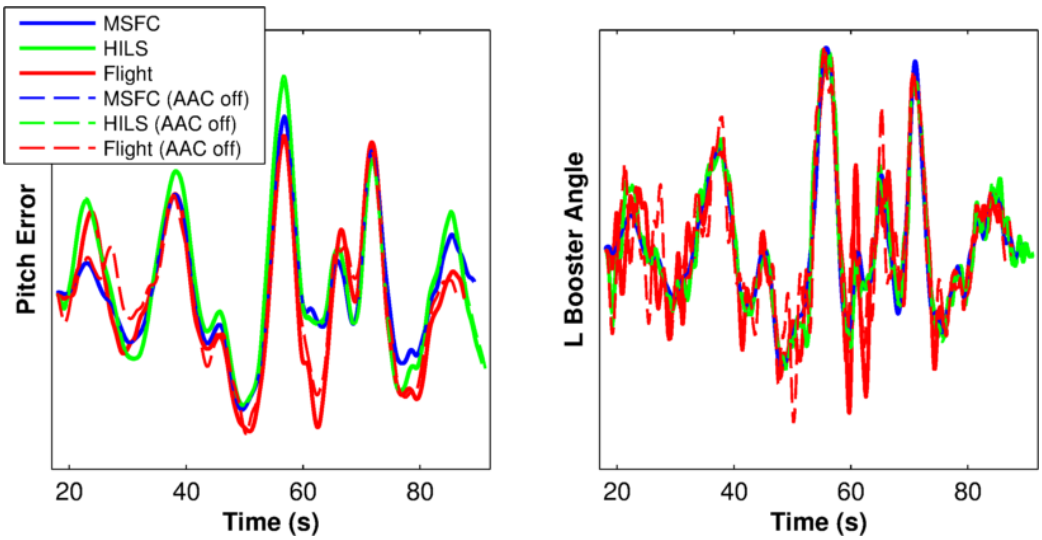

Figure 10. Results for the Nominal SLS Scenario

In the absence of adaptation, the total adaptive gain multiplier, shown in Figure 9, would be unity. The flight test results are consistent with the MSFC simulation and DFRC HILS and show very little adaptation. There is a small but out-of-family decrease in the total loop gain shortly after 60 sec which was caused by a sharp pitch transient induced by the pilot de-throttle command near the crest of the trajectory. The pitch error and left booster angle (illustrating control useage) are shown in

Figure 10 showing excellent matching across simulations and flight as well as very little adaptation. The other test scenarios showed similar results further demonstrating minimal adaptation inside the normal SLS flight envelope and satisfying Objective 1.

5.2 Flight Test Results with Low Performance SLS Scenarios (Objective 2)

The second objective of the research flights was to demonstrate improved performance in an environment where the nominal controller performance is poor. In order to generate these scenarios based on SLS dynamics, key parameters within the model, controller, and environment were modified to create stressing conditions in order to challenge the fixed-gain control system. Table 2 contains for each of the Objective 2 test scnenarios a short description of the SLS conditions. In several cases, slosh was disabled to best isolate the effects of the simulated rigid body or elastic instability. In the cases involving wind disturbances, the aerodynamic instability of the SLS was exaggerated to further stress the baseline attitude controller.

Table 2. Flight Tested Objective 2 Scenarios

TC	Description of SLS Scenario	FT1	FT2	FT3	FT4	FT5
3	Wind shear event		A			
4	Thrust vector control bias		A			
5	Hardover failure of 2 core engines (offset in time)		A		M	M
6	Heavy/slow, wind shear, SRB tailoff thrust imbalance			A		
7	Wind shear event and double hardover failure		A		M	M
14	Low-gain controller, wind shear, 2 hardover failures		A			

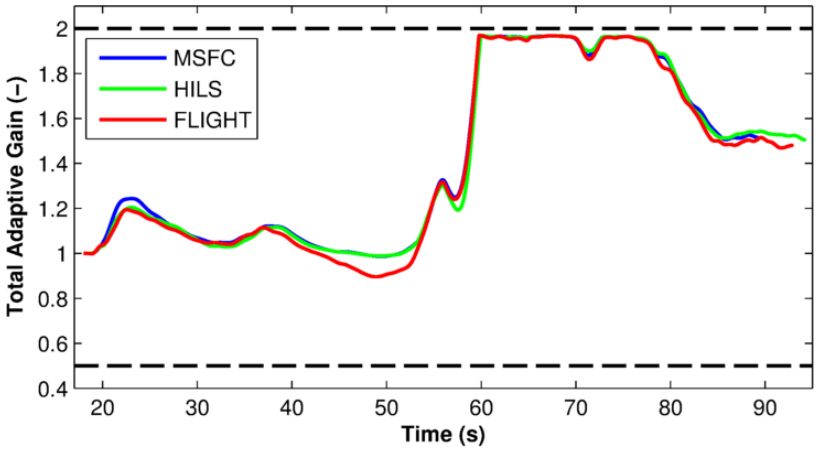

Figure 11. Adaptation of the Total Loop Gain (Low Performance)

All of the Objective 2 scenarios exhibited excellent matching between the MSFC simulated results, the DFRC HILS results, and the flight tests themselves. This is exemplified here through the results of Test Case 7, shown in Figures 11 and 12. This SLS-derived scenario features a wind shear event followed by two core engine hardover failures which would have forced the SLS to exceed the

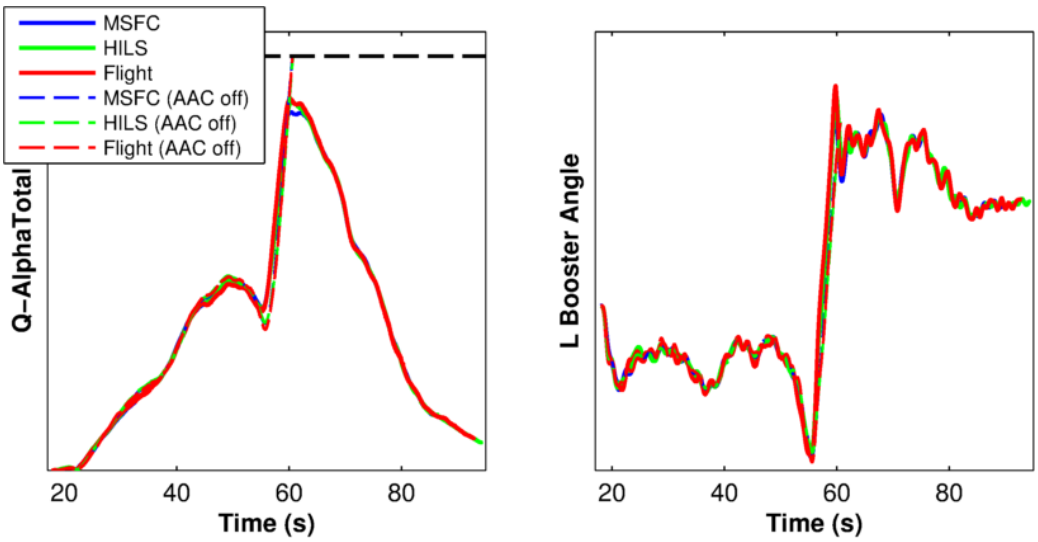

Figure 12. Low Performance Results

physical limits of the structure shortly after 60 sec, where the AAC off test cases are discontinued as observed in 12. In the AAC on versions, the on-line gain adjustment allows the controller to respond more rapidly so that it can keep the SLS within the limits of the structural load indicator without requiring excessive control commands (see Figures 11 and 12). Thus, the AAC algorithm also met its objective of increasing the total loop gain in response to excessive error in the pitch attitude (beyond what would be expected within a normal flight envelope) which corresponds to a successful completion of the research flight objectives. Other test cases which map to this objective reveal similar results thereby increasing the confidence that AAC, as expected, can aid in the performance of the SLS vehicle under anomalous conditions.

5.3 Flight Test Results with Unstable Parasitic Dynamics (Objective 3)

The third flight objective was to demonstrate AAC's ability to restrict unstable, mis-modeled parasitic dynamics to a small-amplitude, non-destructive limit cycle. The test cases associated with this objective are shown in Table 3. Matching of the aircraft's pitch motion to the high frequency, unstable SLS parasitic dynamics for these test cases was considerably more challenging than with the Objective 1 or 2 scenarios. Contributing to the difficulty in matching the high frequency SLS dynamics is that the ability of the NDI to reproduce the content at large magnitudes is sensitive to knowledge of the dynamic pressure which varied from trajectory to trajectory dependent on the pilots' initial conditions. Thus, the resulting amplitude of the pitch attitude and rate are a function of the pilot's initial condition when the experiment is engaged. Furthermore, as fuel is depleted from the aircraft, the inertia properties change significantly leading to greater effectiveness at the beginning of the flight than the end. To better understand these variations,and provide data for the analysis of the NDI performance for high magnitude, high frequency modes, each of the scenarios listed was captured multiple times.

Table 3. Flight Tested Objective 3 Scenarios

TC	Description of SLS Scenario	FT1	FT2	FT3	FT4	FT5
9	Light/fast with slosh instability		A	A		
10	Structural instability		A	A		
15	High-gain controller, slosh instability		A	A		
16	High-gain controller, unstable flex		A	A	MAA	MAA
17	High-gain controller, rigid body instability		A	A	MAA	MAA
20	F/A-18 Structural Mode	ID			S/L	S/L
22	F/A-18 Structural Mode with EGI	ID			S/L	S/L

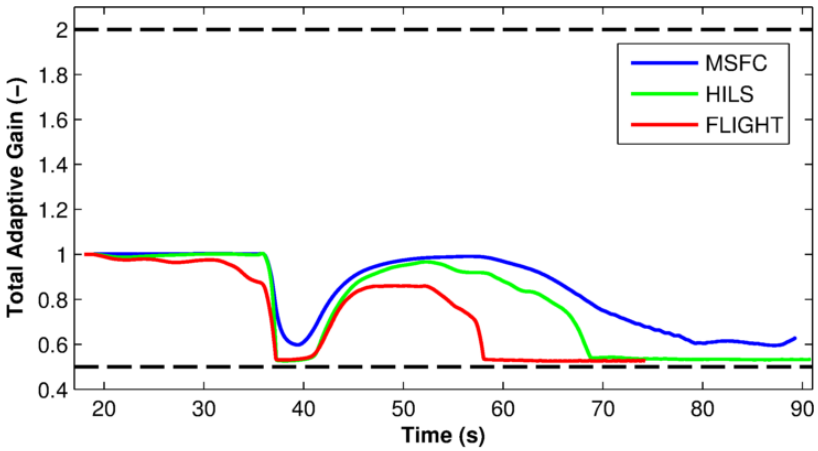

Figure 13. Adaptation of the Total Loop Gain (Fictitiously Unstable Flexible Body Dynamics)

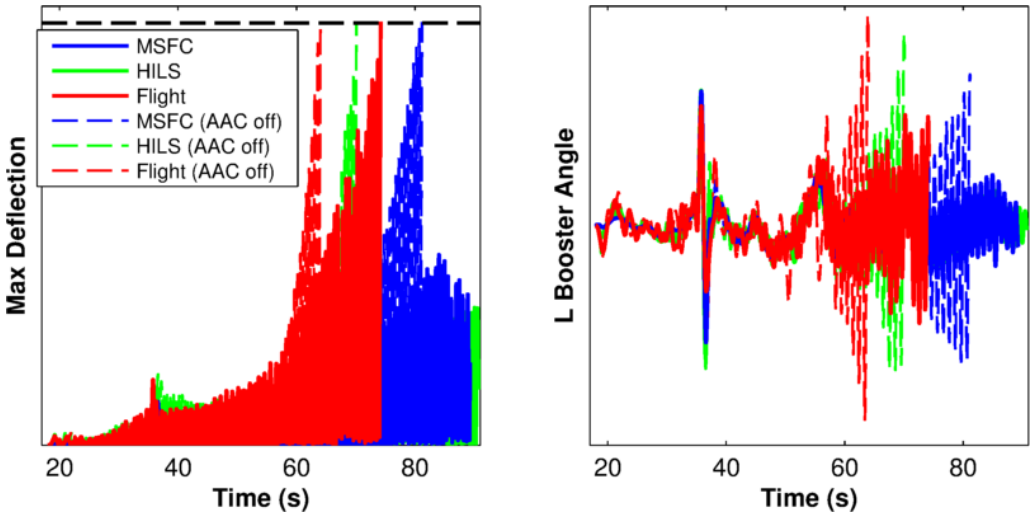

Figure 14. Sample Results for the Fictitiously Unstable Flexible Body Dynamics

Results are shown for test case 16 where the FCS gains were increased and the gain on one of the elastic modes was also increased to simulate an instability. The flex dynamics are applied to the aircraft via the the ailerons, and alternate effectors (primarily stabilators) are used for implementation of the FCS commands. The flaps are mixed in, but to a very small extent. Figure 13 shows the total loop gain at its initial value of 1, then decreasing rapidly at approximately 35 sec when the SLS model disturbance was applied to excite the unstable elastic mode. As the instability grows, the frequency content enters into the SLS control command and the AAC response by decreasing the gain to its limit of 0.5. The vehicle deflection is shown in 14, along with the booster command. The amplitude of the elastic deflection was higher during flight than observed in either simulation due to the effectiveness of the NDI and ailerons at the SLS mode frequency being higher than expected. As a result, the larger amplitude instability could not be be eliminated even with the total loop gain at its minimum value, but it does delay simulated LOV for approximately 10 sec, a significant accomplishment. A similar trend was seen in test case 10 which also used the aircraft's ailerons to provide motion corresponding to simulated flex instability. Test cases 9, 15, and 17, which used alternate control surfaces, were all able to demonstrate recovery (reduction to a low-amplitude limit cycle) through the use of AAC.

5.4 Airframe Structural Mode Identification and Amplification Test (Objective 3)

The Objective 3 test cases for the majority of the research flights demonstrated recovery of unstable SLS structural modes, slosh, or rigid body instabilities as implemented in the SLS reference model within the aircraft's software. This was driven by control surfaces, and measured through the resultant rigid body response of the aircraft. Additional tests were conducted to further demonstrate the ability of the adaptive control to attenuate unfavorable interaction between the control system and the physical F-A/18 structural mode of vibration. During the first research flight, tests were conducted to identify the primary pitch structural mode of the airframe from the symmetric stabilator command to the pitch rate response at each of two sensor packages. During the second series of flights, test cases were flown which intentionally destabilized the closed loop response with the F/A-18 airframe mode and demonstrated the the ability of the adaptive element to suppress the divergent response. For both sets of tests, the baseline F/A-18 filters on the pitch rate feedback to the SLS controller were set to unity while the filters in the FAST NDI were maintained. In addition, the SLS controller attitude error and rate error filters within were set to unity, and the SLS reference model slosh dynamics, flex dynamics, and actuator limits were all disabled. These adjustments yielded a simple system in which the SLS FCS with adaptive element interacts with the FAST NDI and basic F/A-18 airframe.

To identify the structural response, a 60 sec Programmed Test Input (PTI) signal[9] was added to the SLS angular acceleration control command with a frequency range around the expected resonance. The magnitude of the resultant PTI waveform was configurable in flight with subsequent presses of the nose-wheel-steering (NWS) button. The highest magnitude of the five available values corresponded to the point at which the stabiliators were predicted to reach actuator rate saturation. The in-flight adjustability of the test input magnitude allowed for a build-up approach to ensure the safety of the airframe and pilot in the case of unexpectedly high response magnitudes or adverse behavior. For each of the modal identification test segments, the pilot selected the desired PTI magnitude as indicated by the control room, engaged the experiment during straight-and-level flight, and thereafter maintained speed and altitude (constant dynamic pressure) with gentle stick motions. In total, three 60 second segments were flown each with increasing magnitude. The third and largest magnitude showed the predicted stabilator rate limiting. Figure 15 shows the frequency response as

reconstructed from the flight data using the second largest magnitude PTI.

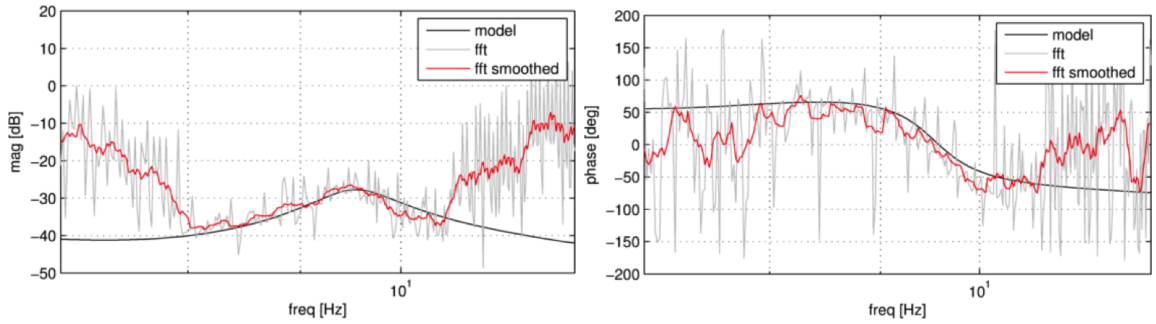

Figure 15. F/A-18 Airframe Mode Reconstructed Frequency Response

After obtaining the reconstructed flight results, a simple second order linear model (parametrized by frequency, damping, gain, and delay) of the structural mode was superimposed with the existing model of the rigid body dynamics and fitted to the flight data. The resulting model (shown by lines "model" in Figure 15) was used to design an eighth order bandpass filter[10] to place in the control path so that the structural mode was amplified to instability but still within the capability of AAC to mitigate the divergent response. The bandpass filter, shown in Figure 16, was placed on the output of the SLS FCS to avoid amplification of sensor noise into the AAC spectral damper and to effect direct frequency shaping of the total system response. To allow fine tuning of the magnitude and phase in-flight, four gain options and five frame delay options were applied in series with the amplification filter.

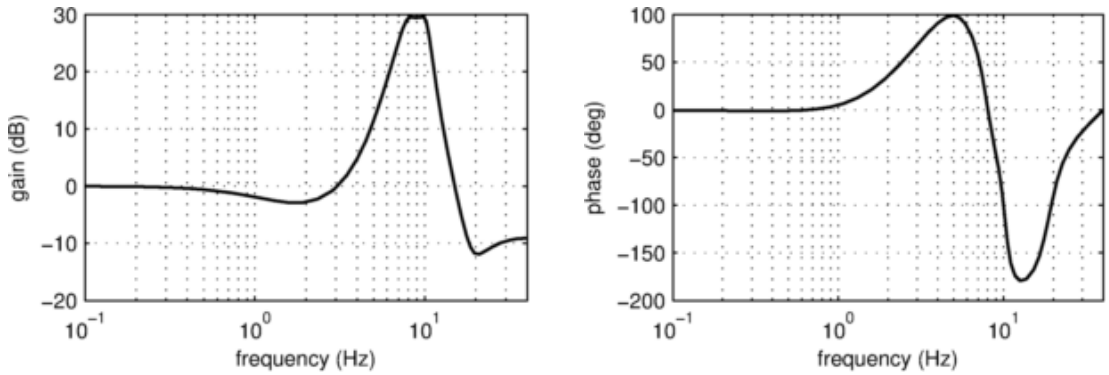

Figure 16. Airframe Resonance Amplification Filter

For the modal amplification test cases, the bandpass filter was applied, and gain delay conditions were configured on flight day to yield a precise structural instability. During the first test segments of the second research flights, the pilot engaged the amplification experiment at the same straight and level flight conditions as were flown during the identification tests. Figure 17 shows the results from the amplification test flown with AAC disabled and AAC enabled. In each case, a short burst of the original PTI signal is scheduled at the 5 sec mark to excite the structural resonance. For the case when AAC is disabled, the symmetric stabiliator response (black line, left plot) quickly diverges until reaching a limit cycle constrained by its maximum rate capability. When AAC is enabled, the

total gain is decreased (red line, right plot) yielding a reduced control response with significantly increased margin from its rate limits. This test case demonstrated, for the first time, the ability of the AAC algorithm to safely recover from an unstable physical structural resonance.

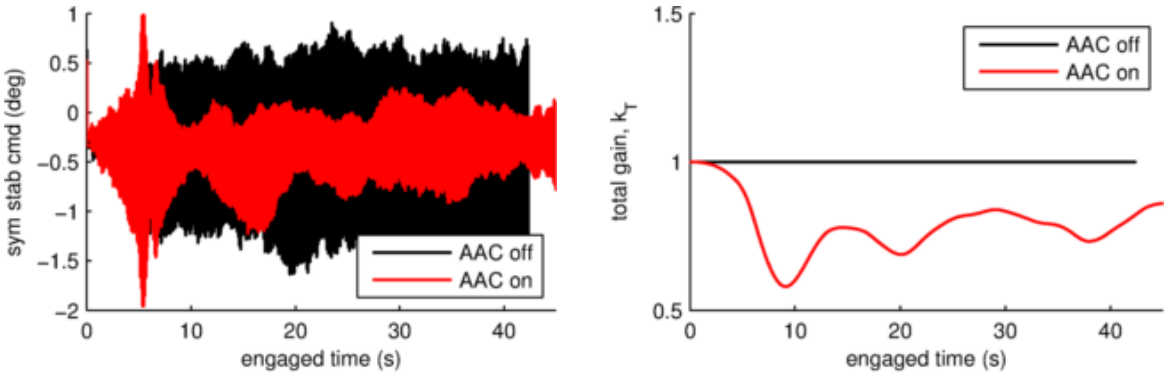

Figure 17. Airframe Structural Mode Recovery Test Case Results

6 CONCLUSION

The ability of the SLS FCS to recover from adverse flight conditions using adaptation has been conclusively demonstrated through a series of flight tests. Many of the simulated flight conditions could not be suitably accommodated in the absence of the adaptive algorithm. The functionality of AAC was as expected in all scenarios, and the flight data matched the DFRC and MSFC simulation results exceptionally well in the low performance and near-nominal test cases. For the Objective 3 cases exhibiting less than a perfect match with the pre-flight simulation, the AAC was still shown to recover from or significantly delay the consequences of severe instability. The great number of successful trajectories demonstrated in this flight test in addition to the millions of simulated trajectories significantly advance the confidence of the SLS Program towards employing the adaptive augmenting control algorithm for the first SLS unmanned mission.

ACKNOWLEDGMENTS

The authors would like to extend their appreciation to those who have supported the initial and continued development of the adaptive augmenting controller, including but not limited to Mark Whorton for casting the vision and initial research towards the development of adaptive control for launch vehicles. Several members of the NASA community also served a critical role in being able to allocate time in the algorithm's initial development phase, providing expert review, gaining support within the NASA community, and obtaining resources toward the flight characterization experiment including John Hanson, Don Krupp, Mark Jackson, Steve Ryan, Dave Edwards, Charlie Hall, Jimmy Compton, Jimmy Jang, Mark West and Garry Lyles.

We would also like to thank the DFRC engineering team, including Chris Miller, Curtis Hanson, pilots Jim ("Clue") Less and David ("Nils") Larson, and many others. In addition, the authors thank our partners Neil Dennehy, Ken Lebsock, Vicki Regenie, Jim Stewart, Steven Gentz, Patricia Pahlavani, and Pam Sparks of the NASA Engineering and Safety Center (NESC). We are also grateful for the funding contribution provided by the Space Technology Mission Directorate towards the completion of this flight campaign.

REFERENCES

[1] J. Hanson, "A Plan for Advanced Guidance and Control Technology for 2nd Generation Reusable Launch Vehicles," in *AIAA Guidance, Navigation, and Control Conference, Monterey, CA, AIAA-2002-4557*, 2002.

[2] J. Orr and T. VanZwieten, "Robust, Practical Adaptive Control for Launch Vehicles," in *AIAA Guidance, Navigation, and Control Conference, Minneapolis, MN, AIAA-2012-4549*, August 2012.

[3] J. Wall, J. Orr, and T. VanZwieten, "Space Launch System Implementation of Adaptive Augmenting Control," in *AAS Guidance, Navigation, and Control Conference, Breckenridge, CO*, 2014.

[4] J. Orr, J. Wall, T. VanZwieten, and C. Hall, "Space Launch System Ascent Flight Control Design," in *AAS Guidance, Navigation, and Control Conference, Breckenridge, CO*, 2014.

[5] C. Hanson, "Capability Description for NASA's F/A-18 TN 853 as a Testbed for the Integrated Resilient Aircraft Control Project," Tech. Rep. DFRC-IRAC-CAP-002, NASA Dryden Flight Research Center, January 2009.

[6] C. Miller, "Nonlinear Dynamic Inversion Baseline Control Law: Architecture and Performance Predictions," in *AIAA Guidance, Navigation, and Control Conference, Portland, Oregon*, 2011.

[7] C. Miller, "Nonlinear Dynamic Inversion Baseline Control Law: Flight-Test Results for the Full-scale Advanced Systems Testbed F/A-18 Airplane," in *AIAA Guidance, Navigation, and Control Conference, Portland, Oregon*, 2011.

[8] J. Orr, M. Johnson, J. Wetherbee, and J. McDuffie, "State Space Implementation of Linear Perturbation Dynamics Equations for Flexible Launch Vehicles," in *AIAA Guidance, Navigation, and Control Conference, Chicago, Illinois, AIAA-2009-5962*, 2009.

[9] V. Klein and E. A. Morelli, *Aircraft System Identification: Theory and Practice*. AIAA Education Series, 2006.

[10] J. Orr, "Optimal Recursive Digital Filters for Active Bending Stabilization," in *AAS Guidance, Navigation, and Control Conference, Breckenridge, CO*, 2013.